

# Inter-Harmonics in Voltage-Sourced Converters based High Voltage Direct Current Systems

Phuchuy Nguyen<sup>\*1</sup>, Minxiao Han<sup>1</sup>, Wenli Yan<sup>2</sup>

<sup>1</sup>School of Electrical and Electronic Engineering

<sup>2</sup>School of Mathematical & Physical Science, North China Electric Power University, Beijing, China, 010-51971645

\*Corresponding author, e-mail: huynp@epu.edu.vn

## Abstract

*Voltage-Sourced Converter (VSC) is the main component in a VSC-based High Voltage Direct Current (HVDC) system. In addition to the characteristic harmonics, the inter-harmonics could be originated from the characteristic of each converter working at different modulation frequencies, or from a distorting frequency on one or both ac (or dc) systems. The space vector representation of VSC's switching functions is used as a tool for analyzing and giving the understanding how the inter-harmonics appear. Based on the methodological analysis, simulation models were built and implemented using SimPowerSystems in MATLAB for cases. The simulation results show that, a series of inter-harmonics is produced tend to be dominant in low-frequency range, especially the negative-sequence inter-harmonics which have lower frequencies than the fundamental. This elaborate understanding of VSC-based HVDC system's inter-harmonic characteristic could be beneficial to harmonic measurement and mitigation control.*

**Keywords:** voltage sourced converter, VSC-based HVDC, inter-harmonic, switching function

**Copyright © 2015 Institute of Advanced Engineering and Science. All rights reserved.**

## 1. Introduction

The Voltage-Sourced Converter based High Voltage Direct Current (VSC-based HVDC) systems have been utilized in power system for many years from the first test in 1997. Some advantages of VSC-based HVDC include [1]: Independent control of active and reactive power; Possibility to supply passive weak networks and back-start capability; High dynamic performance; Multi-terminal possibility.

However, VSC-based HVDC producing harmonics on both ac-side and dc-side is inherent by the VSC itself, called characteristic harmonics, and will interact with harmonic distortions already existed in the system. The characteristic harmonics of VSC are directly associated with the type of VSC technologies, modulation techniques and the switching frequency [2]. When the ac supply is unbalanced or one side of VSC contains background harmonics, there are non-characteristic harmonics on both ac- and dc-side of the VSC [3, 4]. Inter-harmonics are the non-integral non-characteristic harmonics, which are caused by an AC/DC/AC system operating with different frequencies on the both ac-sides [5]. Well understanding these harmonics will contribute to establish adequate approaches to harmonic eliminating, improving the system performance.

Several works have studied harmonic interactions between the two sides of the converter and through the dc-link of HVDC [3-8]. In [3], the harmonic transfer characteristic of a current source converter based HVDC has been analyzed. In the case of the two ac systems are asynchronous, a background harmonic from one end ac system will be transferred to the other end and produces two inter-harmonics. For the VSC-based HVDC scheme, a non-integral harmonics on the dc-side will cause two inter-harmonics on the ac-side [4]. The amplitudes of inter-harmonics depend on the impedances on both ac- and dc-side of the converter [6, 7]. For a practical project in [8], harmonic emission from wind turbines, which contains VSCs, has been measured and showed that groups of inter-harmonics appearing in the output current spectrum. These inter-harmonics are mainly gathered and significant in the low-frequency range.

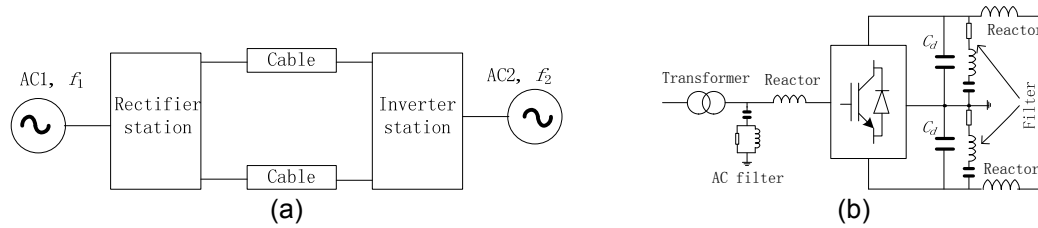


Figure 1. Model system for analyzing inter-harmonic characteristic. (a) System block diagram; (b) Rectifier/Inverter station

The harmonic transfer characteristic of VSC is investigated in this paper, which considers both the fundamental and high-order switching components of the VSC's switching functions. This is a contrast to all previous analyses which have just considered the fundamental switching component. In fact, the high-order switching components have significant effects on the amplitude and the sequence of harmonics. By using the switching functions of VSC represented in space vector form, the origin and characteristic of inter-harmonic on VSC-based HVDC systems are also investigated. In an asynchronous HVDC connection whose ac grids differ in frequency, one end converter's dc-side characteristic harmonics will be the ripples to the other end converter. Consequently, these ripples could induce inter-harmonics on the ac systems. The distorting in frequency of one ac system could also cause inter-harmonics to be produced in the system also. Furthermore, a background harmonic in one end ac system will be transferred to the other end ac system and produces a series of inter-harmonics.

Under the mathematical analysis, the inter-harmonic characteristic can be studied by using the simulation model in Figure 1. The system's parameters may be changed in corresponding to each case of study. In converter stations, reactors are installed on the both sides of the converters. The transformer winding is Yn/Y connection type where the Y winding is on the converter-side, resulting in decoupling the ac system from the triple harmonics produced by the converter. The ac high-pass filter group is an essential part of the scheme, located between the converter transformer and the converter reactor for improving filtering characteristic. The dc-side of the VSC uses reservoir dc capacitors to equalize dc voltage, enhance the system dynamics, and reduce the dc-side voltage ripples, where the most dominant 3<sup>rd</sup> harmonic will be filtered out by the 3<sup>rd</sup> order tuned filters.

## 2. Research Method

### 2.1. VSC's Operation Principle

In Figure 2, a three-level NPC VSC forces the ac-side voltage to a certain value determined by the given switching functions. Corresponding to three voltage levels, the switch of phase  $x$  takes the value  $k_x=1$ ,  $k_x=0$ , and  $k_x=-1$ , respectively switching to the positive dc pole, the "midpoint," and the negative dc pole. For the VSC using pulse-width modulation (PWM) technique, the  $k_x=1$  and  $k_x=-1$  correspond to the positive and negative half cycle modulation wave, respectively.

In order to reduce harmonic level, the naturally sampled phase disposition PWM is adopted. The switching states of valves are defined by comparing the sinusoidal modulation wave with two high frequency triangular carriers. Using the double Fourier analysis, the expression of switching function of phase  $x$  (with " $x = a, b, c$ " also used for all following equations) of a three-level converter in time domain is given by the following Equation [2]:

$$k_x(t) = M \cos(\omega_1 t + \theta_x) + \frac{2}{\pi} \sum_{m=2,4,6,\dots}^{\infty} \frac{1}{m} \sum_{n=-\infty}^{+\infty} \left[ J_{2n+1}(m\pi M) \cos n\pi \cdot \cos(m(\omega_c t + \delta) + [2n+1](\omega_1 t + \theta_x)) \right] + \frac{8}{\pi^2} \sum_{m=1,3,5,\dots}^{\infty} \frac{1}{m} \sum_{n=-\infty}^{+\infty} \left[ J_{km} \cos n\pi \cdot \cos(m(\omega_c t + \delta) + 2n(\omega_1 t + \theta_x)) \right] \quad (1)$$

Where:  $M$  is the modulation index;  $\omega_1$  is the frequency of the modulation wave;  $\omega_c$  is the frequency of the carrier wave;  $m$  is the group index (multiple of switching frequency);  $n$  is the

sideband harmonic index from each group;  $\theta_x$  is the modulation wave phase shift for each phase  $x$ ;  $\delta$  is the carrier wave phase shift;  $J_{2n+1}, J_{2k-1}$  is the first kind Bessel functions (see Appendix A); and  $J_{km}$  is defined in (2).

$$J_{km} = \sum_{k=1}^{\infty} J_{2k-1}([2m-1]\pi M) \frac{(2k-1)}{(2k+2n-1)(2k-2n-1)} \tag{2}$$

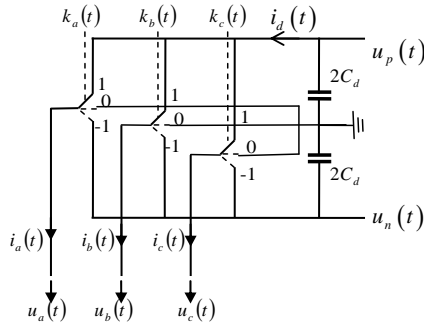


Figure 2. Three-level voltage sourced converter phase quantities.

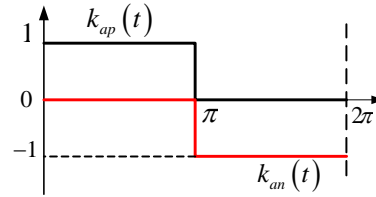


Figure 3. Step functions of phase a

The switching functions are used to determine the relationships between the both side quantities of the converter. Generally, these relationships can be expressed in (3) for phase  $x$ .

$$u_x(t) = k_x(t) \cdot u_{xd}(t) \tag{3}$$

Where:

$$u_{xd}(t) = [u_p(t) \cdot k_{xp}(t) + u_n(t) \cdot k_{xn}(t)] \tag{4}$$

In (4),  $u_p(t)$  and  $u_n(t)$  are dc-side positive and negative pole voltages, respectively;  $k_{xp}(t)$  and  $k_{xn}(t)$  are step functions corresponding to each half cycle of phase  $x$  modulation wave, as shown in Figure3.

It can be seen that, for phase  $a$ ,  $k_{ap}(t) - k_{an}(t) = 1$  and  $[k_{ap}(t) + k_{an}(t)]$  is a periodic function, and thus can be expanded by a Fourier series as [6]:

$$[k_{ap}(t) + k_{an}(t)] = \frac{4}{\pi} \sum_{h=1,3,5,\dots}^{\infty} \frac{1}{h} \sin \frac{h\pi}{2} \cos(h\omega_1 t) \tag{5}$$

Adding  $-2\pi/3$  and  $2\pi/3$  to the phase angle of each harmonic component in (5) will derive the correspondence forms of phase  $b$  and  $c$ , respectively.

The dc-side current on the positive dc pole is established in (6).

$$i_d(t) = [k_a(t)i_a(t) + k_b(t)i_b(t) + k_c(t)i_c(t)] / 2 \tag{6}$$

In the case of  $u_p(t) = -u_n(t) = u_d(t)/2$ , the relationships between ac- and dc-side quantities of VSC, without the zero sequence components, now can be determined in the general formula of the space vector [4]:

$$\begin{cases} \bar{u}_v(t) = \bar{K}(t) \cdot u_d(t) / 2 \\ i_d(t) = \frac{3}{4} \text{Re} \left[ [\bar{K}(t)]^* \bar{i}_v(t) \right] \end{cases} \tag{7}$$

Where:  $\bar{u}_v(t)$ ,  $\bar{i}_v(t)$  are space vector of ac-side voltage and current respectively;  $u_d(t)$ ,  $i_d(t)$  are the dc-side voltage and current, respectively;  $\bar{K}(t)$  is the space vector of three-sinusoidal switching functions.

## 2.2. Space Vector Representation of Switching Functions

As can be seen from (1), the first term gives the fundamental component of switching function. Its amplitude just is dependent on the modulation index, but is independent of the frequency index,  $m_f = \omega_c/\omega_1$ , and carrier phase shift. The amplitudes of other harmonics depend on the characteristic of the Bessel function, which are equal for two sideband harmonics on opposite sides of the center-placed harmonic in each group.

In each group of carrier sidebands, the high-order switching components satisfy  $m \cdot m_f + n = 3i = N_{mn}^0$ , where  $i$  is an integer, are called zero-sequence switching components. It is clear from (6) that the dc current is not affected by the zero sequence switching components. The high-order switching components satisfy  $m \cdot m_f + n = 3i + 1 = N_{mn}^+$  are called positive-sequence switching components. And the other high-order switching components satisfy  $m \cdot m_f + n = 3i - 1 = N_{mn}^-$  are called negative-sequence switching components. As a result, the space vector of switching functions is composed of three components expressed as the following equation:

$$\bar{K}(t) = \bar{K}_1(t) + \sum_{m=1}^{\infty} \sum_{n=-\infty}^{+\infty} \bar{K}_{mn}^+(t) + \sum_{m=1}^{\infty} \sum_{n=-\infty}^{+\infty} \bar{K}_{mn}^-(t) \quad (8)$$

Where:

$$\begin{cases} \bar{K}_1(t) = M e^{j\omega_1 t} \\ \bar{K}_{mn}^+(t) = \hat{K}_{mn}^+ e^{jN_{mn}^+ \omega_1 t} \\ \bar{K}_{mn}^-(t) = \hat{K}_{mn}^- e^{-jN_{mn}^- \omega_1 t} \end{cases} \quad (9)$$

In (9),  $\hat{K}_{mn}^+$  and  $\hat{K}_{mn}^-$  are the amplitudes of the positive- and negative-sequence switching components, respectively. It is clear that, the zero-sequence switching components, which has triple orders, does not appear.

## 2.3. Ripples on DC-side caused by Harmonics Transferred from AC-side

Practically, many VSC-based HVDC systems are asynchronous interconnections whose ac grids have different fundamental frequencies. Moreover, for the synchronous interconnection between two identical frequency ac systems, there may be distorting in frequency in operation. For these schemes, the dc-side characteristic harmonics of one end converter could be acted as the dc-side ripples to the converter at the opposite end. Consequently, the both end converters will operate to cause the different harmonic spectrum on their both ac- and dc-side.

Assuming ac-side currents of the converter 1 superimpose harmonic components expressed in the space vector form as:

$$\bar{i}_{vh}(t) = \hat{i}_h^+ e^{j\omega_h t} + \hat{i}_h^- e^{-j\omega_h t} \quad (10)$$

The first part in (10) is the positive-sequence harmonic, and the second is the negative-sequence harmonic. Substituting (10) to the second equation in (7) with the expression of switching function as (8), we get:

$$i_{dh}(t) = i_{d1h}(t) + \sum_{m=1}^{\infty} \sum_{n=-\infty}^{+\infty} i_{dmnh}^+(t) + \sum_{m=1}^{\infty} \sum_{n=-\infty}^{+\infty} i_{dmnh}^-(t) \quad (11)$$

Where:

$$\begin{cases} \hat{i}_{d1h}^-(t) = \frac{3M}{4} \operatorname{Re} \left[ \hat{i}_h^+ e^{j(\omega_h - \omega_1)t} + \hat{i}_h^- e^{-j(\omega_h + \omega_1)t} \right] \\ \hat{i}_{dmh}^+(t) = \frac{3\hat{K}_{mn}^+}{4} \operatorname{Re} \left[ \hat{i}_h^+ e^{-j(N_{mn}^+ \omega_1 - \omega_h)t} + \hat{i}_h^- e^{-j(N_{mn}^+ \omega_1 + \omega_h)t} \right] \\ \hat{i}_{dmh}^-(t) = \frac{3\hat{K}_{mn}^-}{4} \operatorname{Re} \left[ \hat{i}_h^+ e^{j(N_{mn}^- \omega_1 + \omega_h)t} + \hat{i}_h^- e^{j(N_{mn}^- \omega_1 - \omega_h)t} \right] \end{cases} \quad (12)$$

In the case of a balanced harmonic, the ac-side has just only the positive or negative-sequence harmonic. Equation (12) shows that, only one sideband harmonic to be produced on the dc-side for each sequence of the harmonic. The interaction of the positive-sequence switching components (including the fundamental component) contrast with the negative-sequence switching components; the positive-sequence harmonic offers lower order sideband, while the negative-sequence harmonic offers higher order one.

When the ac-side has an unbalanced harmonic, it has both the positive- and negative-sequence components as in (10). Therefore, there will be two sideband harmonics on the dc-side, but their amplitude depends on the amplitude of the origin components on the ac-side, respectively.

#### 2.4. Inter-harmonics on the AC-side caused by the DC-link ripples

Assume that the dc-side voltage comprises a ripple with angle frequency  $\omega_r$ , which is not an integer of the fundamental, written in the form as:

$$u_{dr}(t) = \hat{u}_{dr} \cos(\omega_r t) = \hat{u}_{dr} (e^{j\omega_r t} + e^{-j\omega_r t}) / 2 \quad (13)$$

Under the interaction of the zero-sequence switching components, the dc-side harmonic voltage transfer through VSC can be explained in (14) for example of phase a output voltage:

$$\begin{aligned} u_{a,mnr}^0(t) &= \hat{K}_{mn}^0 \cos(N_{mn}^0 \omega_1 t) \frac{\hat{u}_{dr} \cos(\omega_r t)}{2} \\ &= \frac{\hat{K}_{mn}^0 \hat{u}_{dr}}{4} \left[ \cos(N_{mn}^0 \omega_1 + \omega_r)t - \cos(N_{mn}^0 \omega_1 - \omega_r)t \right] \end{aligned} \quad (14)$$

These additional harmonics are all zero-sequence harmonics, and therefore, they will not appear in line voltage.

For the other switching components, substitute (13) to the first equation in (7) with the expression of switching function as (8), we get:

$$\bar{u}_{Vr}(t) = \bar{u}_{1r}(t) + \sum_{m=1}^{\infty} \sum_{n=-\infty}^{+\infty} \bar{u}_{mnr}^+(t) + \sum_{m=1}^{\infty} \sum_{n=-\infty}^{+\infty} \bar{u}_{mnr}^-(t) \quad (15)$$

Where,

$$\begin{cases} \bar{u}_{1r}(t) = \frac{M}{4} \cdot \hat{u}_{dr} (e^{j(\omega_r + \omega_1)t} + e^{-j(\omega_r - \omega_1)t}) \\ \bar{u}_{mnr}^+(t) = \frac{\hat{K}_{mn}^+}{4} \cdot \hat{u}_{dr} (e^{j(N_{mn}^+ \omega_1 + \omega_r)t} + e^{j(N_{mn}^+ \omega_1 - \omega_r)t}) \\ \bar{u}_{mnr}^-(t) = \frac{\hat{K}_{mn}^-}{4} \cdot \hat{u}_{dr} (e^{-j(N_{mn}^- \omega_1 + \omega_r)t} + e^{-j(N_{mn}^- \omega_1 - \omega_r)t}) \end{cases} \quad (16)$$

As can be seen from (16), there are two sideband inter-harmonics in the ac-side of the VSC, corresponding to a ripple on the dc-side. Under the interaction of the fundamental switching component, the higher order inter-harmonic is a positive-sequence component, and

the lower order is a negative-sequence one if  $\omega_r > \omega_1$ , and vice versa. Whereas, under the interaction of the high-frequency switching components, if the frequency of the dc-side ripple is smaller than the frequency of switching components, the sequence of the two-sideband inter-harmonics on ac-side is the same sequence as the switching components.

### 2.5. Inter-harmonics on the AC-side caused the DC-capacitor Ripples

In the three-level NPC VSC, the midpoint current contains large third-harmonic component, causing the third-harmonic voltage (the ripple) on the dc capacitor. This voltage harmonic in turn results in low-order voltage harmonics on the ac-side of the converter [9]. Moreover, the midpoint current could flow through the earth return path between two ends of the dc-link. In the case of the two ac systems have different frequencies, low-order inter-harmonics may be produced on one end ac system because of the dc capacitor ripples of the other end. Assuming that the ripple on the dc capacitor at the end 2 of the dc-link caused by the midpoint current from the end 1 is expressed as (17):

$$u_{3r}(t) = U_{3r} \cos(3\omega_1 t + \xi) \quad (17)$$

The dc positive and negative pole voltages now can be written as the following equation:

$$\begin{cases} u_p(t) = U_d / 2 + U_{3r} \cos(3\omega_1 t + \xi) \\ u_n(t) = -U_d / 2 + U_{3r} \cos(3\omega_1 t + \xi) \end{cases} \quad (18)$$

Just considering the second parts in (18) and substitute them into (4) for the converter 2, we get for the case of phase a:

$$u_{ad}(t) = \frac{4U_{3r}}{\pi} \sum_{h=1,3,5,\dots}^{\infty} \frac{1}{h} \sin \frac{h\pi}{2} \cos([3\omega_1 \pm h\omega_2]t + \xi) \quad (19)$$

Under the interaction of the fundamental switching component, the phase a output voltage on the ac system 2 could be achieved by substituting (19) into (3), expressed in (20).

$$u_{a2}(t) = \frac{MU_{dc}}{2} \cos(\omega_2 t) + \frac{MU_{3r}}{\pi} \sum_{h=1,3,5,\dots}^{\infty} \frac{1}{h} \sin \frac{h\pi}{2} \cos([3\omega_1 \pm h\omega_2 \pm \omega_2]t + \xi) \quad (20)$$

From (20), the additional inter-harmonics may have smaller frequency than the fundamental which could damage rotating machine connected to the system, especially in case of negative-sequence harmonics.

### 2.6. Inter-harmonics under Unsymmetrical Conditions

When the point of common coupling (PCC) on the ac system 1 is subjected to single phase-to-ground fault, the HVDC system will operate under unbalanced conditions, and VSC is quite sensitive to the negative-sequence component in the ac voltage [10].

Based on the theory of symmetrical components, an unbalanced three-phase current comprise three balanced components of positive-, negative- and zero-sequence components. The mathematical expression of phase x current is the following equation:

$$i_{sx}(t) = \hat{I}_s^+ \cos(\omega_1 t + \theta_x) + \hat{I}_s^- \cos(\omega_1 t + \varphi + \theta_x) + i_s^0(t) \quad (21)$$

Where  $\hat{I}_s^+$ ,  $\hat{I}_s^-$  are the current amplitude of positive- and negative-sequence component, respectively;  $\varphi$  is the phase angle of the negative-sequence component, relative to the positive-sequence component.

The space vector corresponding to three-phase current without the zero-sequence component is:

$$\bar{i}_s^-(t) = \hat{I}_s^+ e^{j\omega_1 t} + \hat{I}_s^- e^{-j(\omega_1 t + \varphi)} \quad (22)$$

Equation (22) has a similar form as (10) for unbalanced harmonics. As a result, a series of ripples will be induced on the dc-side of the converter where the component with frequency  $2\omega_1$  is dominant. Again, this dominant component is conveyed to the ac system 2 to produce a series of inter-harmonics, where the negative-sequence and positive-sequence components have frequencies at  $2\omega_1 - \omega_2$  and  $2\omega_1 + \omega_2$ , respectively, are dominant.

### 3. Simulation and Result Analysis

Simulation models were set up for the VSC-based HVDC system on Figure 1 using SimPowerSystems in Matlab. In each model, the sending end VSC was modeled to operate as power dispatcher while the receiving end VSC was modeled to operate as dc voltage regulator and reactive power controller. In each VSC station, the VSC is a 6-IGBT bridge three-level NPC converter. The VSCs adopt the SPWM modulation technique. The frequency of the triangle carrier wave is 27 times of the fundamental frequency. The parameters of each model are given in the Appendix.

For acceptable correctness of measurement both harmonics and inter-harmonics, Fourier analysis was implemented with a number cycle windows was chosen how to get a suitable resolution spectrum for both two systems. For example, according to IEC-61000-4-7 standard, a 10 (for 50 Hz systems) or 12 (for 60 Hz systems) cycle windows was chosen, therefore a spectrum with 5 Hz resolution will be achieved [5].

#### 3.1. Case 1: Two AC Systems Operate at 50 Hz

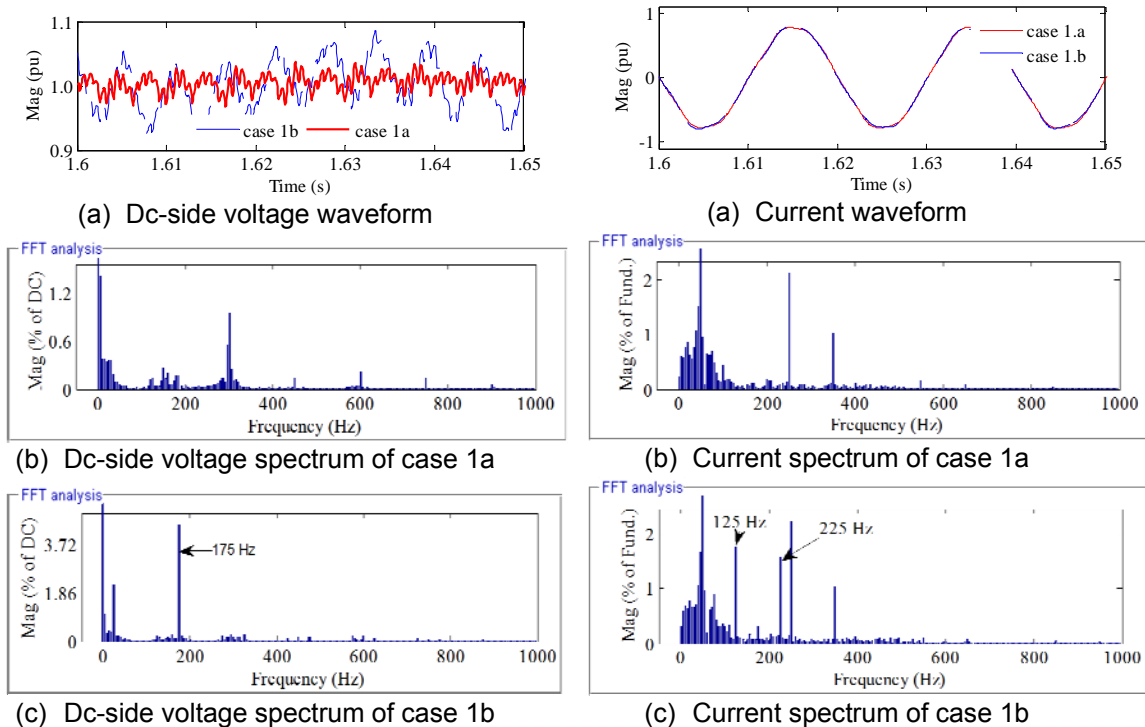


Figure 4. Case 1: DC-side voltage

Figure 5. Case 1: ac system 2 phase current

The first case is the base-case giving a comparative view to the other cases. As can be seen from (1), the output voltage of the VSC will have the fundamental component and the carrier multiple sidebands. Because of the ac high-pass filters, the harmonic orders equal to or higher than 27 significantly suppressed. Therefore, the phase current was just measured up to 1000 Hz in all cases. The spectrum of dc-side voltage and phase current of ac system 2 (the current flows to the PCC point from the system) are represented in Figure 4 and Figure 5. The

first example in this case is called case 1a assuming that the two ac systems have no distortions. The dc-side voltage and ac system 2 phase current have quite low levels. It can be seen from Fig.5b, the ac system 2 phase current includes the 5<sup>th</sup> and 7<sup>th</sup> harmonics. These harmonics are caused by dc-capacitor ripples when the two ac systems operate at the same frequencies (as shown in (20)).

In the second example (called case 1b), the ac system 1 was assumed to have a distortion with a 10% negative-sequence component at 125 Hz. As a result, the dc-side had induced inter-harmonics causing dc-side voltage to be distorted (Figure 4a) with the dominant at 175 Hz (Figure 4c). This inter-harmonic in turn dominantly resulted in the low frequency range of the ac system 2 a same inter-harmonic to the origin at 125 Hz and a new inter-harmonic at 225 Hz (Figure 5c). The waveforms of the ac system 2 phase currents in these two examples were similar.

### 3.2. Case 2: DC Capacitors Effect Inter-harmonic Characteristic of the System

In this case, the simulation model was similarly built as the case 1, except that the ac system 2 operates at 60 Hz. As above mention, the dc-side of 50 Hz-side converter will contain its own characteristic harmonics, but they are ripples to the 60 Hz-side converter. These ripples, again, are transferred to the ac-side of this converter to produce a non-characteristic harmonics including inter-harmonics. However, the magnitudes of these inter-harmonics are much smaller than the fundamental.

As the analysis in the section 2.5, the inter-harmonics on the ac systems could be originated from the dc capacitors. Figure 6 illustrates the effect of dc capacitors without and with third-harmonic filters on the dc-side. Clearly, some low-frequency inter-harmonics produced if third-harmonic filters were not installed. The simulations gave inter-harmonics were agreed with the analytical results from (20), which are 30 Hz, 90 Hz, 210Hz, 270 Hz, 330 Hz, 390 Hz, etc. (Figure 6b). This inter-harmonics disappeared with third-harmonic filters (Fig.6c), resulted in a smoother current waveform as shown in Figure 6a.

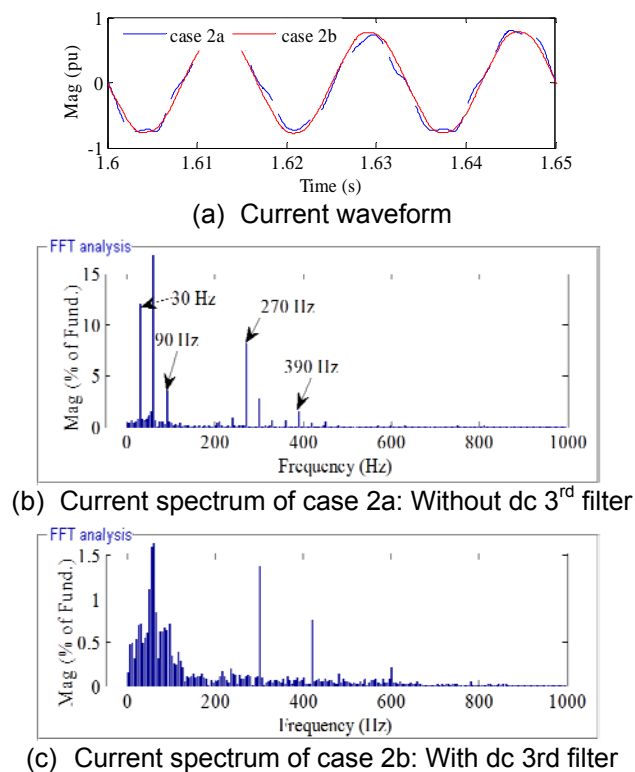


Figure 6. Case 2: the phase current of the ac system 2 under the effect of dc capacitors

### 3.3. Case 3: AC System 1 Includes Unbalanced Harmonic

The simulation model in this case is the model in case 2 with the installation of dc third-harmonic filters. The inter-harmonic level could be larger if one end ac system comprises of the background harmonics. Injecting to the ac system 1 a 10% of unbalanced 2<sup>nd</sup> harmonic (100 Hz), the dc-side voltage and ac system 2 phase current were measured for spectra analyzing. As results, the dc-side was induced a series of harmonics where the 1<sup>st</sup> (50 Hz) and the 3<sup>rd</sup> (150 Hz) harmonics are the dominant ones (Figure 7b). They play the role of inter-harmonics to the 60 Hz-side converter. Analytically, under the interaction of the fundamental switching component, there are inter-harmonics at 10 Hz, 90 Hz, 110 Hz, and 210 Hz in low-frequency range of the ac system 2 (Figure 8b). In addition, there were multiple inter-harmonics produced, because of the interaction of other high-order switching components.

### 3.4. Case 4: Unsymmetrical AC System

In this last case, a single phase-to-ground fault was investigated instead of background harmonic in the case 3.

A fault occurred on the ac system 1 resulting inter-harmonics to be produced in the dc-link and the ac system 2. Figure 7c shows the simulation result in corresponding to the methodological analysis in section 2.6 with 100 Hz ripple on the dc-side. Consequently, there were two induced inter-harmonics with frequencies at 40 Hz and 160 Hz (Figure 8c). Notably, the 40 Hz inter-harmonic is the negative-sequence component smaller than the fundamental one. If a series resonance at this frequency occurs, a modest inter-harmonic voltage is seemed drastically to amplify the inter-harmonic current, damaging the rotating machine connected to the ac system 2.

Although the dc-side voltage in the case 3 was largely distorted in comparison with the case 4 (Figure 7a), the ac system 2 phase currents in both cases were similar (Figure 8a).

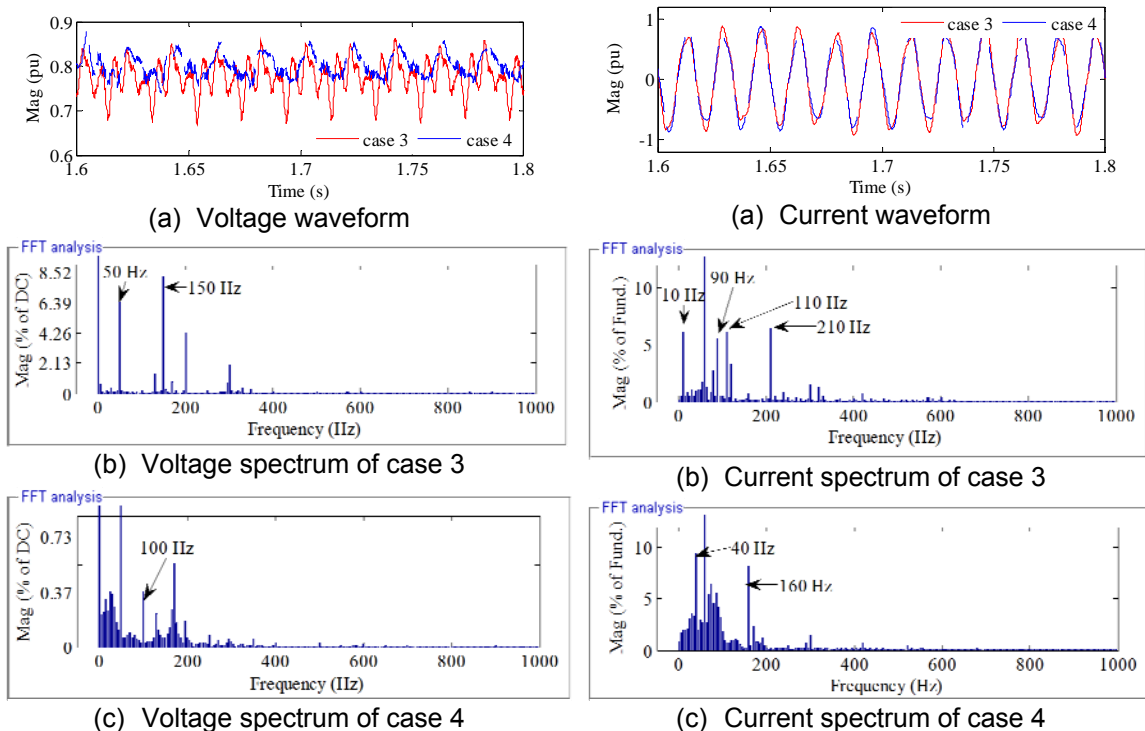


Figure 7. Dc-side voltage when the ac system 1 (50 Hz) has unbalanced 2<sup>nd</sup> harmonic (case 3), and unsymmetrical fault (case 4).

Figure 8. The phase current of the ac system 2 when the ac system 1 (50 Hz) has unbalanced 2<sup>nd</sup> harmonic (case 3), and unsymmetrical fault (case 4).

## 4. Conclusion

The space vector representation of VSC's switching functions is a straightforward tool to

study harmonic interaction. From that, the origin of inter-harmonics in VSC-based HVDC systems was investigated and classified as:

- (1) Resulting from the characteristic of each converter in asynchronous connection;
- (2) Resulting from a distorting frequency;
- (3) Resulting from unsymmetrical fault or unbalance;

In all cases, there was a series of inter-harmonics produced, which is because of the interaction of both fundamental and carrier sideband (high-order) switching components. For confirmation, the simulation models were set up to implement, and giving results agreed with the theoretical analyses. In corresponding to the results, the effect of dc capacitors is significant in raising a series of low-frequency inter-harmonics.

It has to put attention to the inter-harmonics whose frequencies are lower than the fundamental, especially if they are negative-sequence components. These inter-harmonics could seriously damage the rotating machines connected to the system.

### References

- [1] P Jiuping, R Nuqui, K Srivastava, et al. *AC Grid with Embedded VSC-HVDC for Secure and Efficient Power Delivery*. Proceedings of the IEEE Energy 2030 Conference (ENERGY 2008), Atlanta, GA, 2008; 1-6
- [2] Stamatios K. Kartalopoulos et al. *Pulse Width Modulation for Power Converters*. New Jersey: IEEE Press. 2003.
- [3] Lihua Hu, Robert Yacamini. Harmonic Transfer through Converters and HVDC links. *IEEE Trans. Power Electronics*. 1992; 7(3): 514–524
- [4] Ying Jiang, Ake Ekstrom. General Analysis of Harmonic Transfer through Converters. *IEEE Trans. Power Electronics*. 1997; 12(2): 287–293
- [5] EW Gunther. *Inter-harmonics in power systems*. Proceedings of the IEEE Power Engineering Society Summer Meeting, Vancouver, BC. 2001; 2: 813-817.
- [6] L Hu, R Yacamini. *Calculation of harmonics and inter-harmonics in HVDC schemes with low dc-side impedance*. Proceedings C of IEE Generation, Transmission and Distribution. 1993; 140: 469-476.
- [7] Liangxiang Tang, Boon-Teek Ooi. *Converter Nonintegral Harmonics from AC network Resonating with DC Network*. Proceedings of the IEEE Industry Applications Soc. Conference. 2001; 4: 2186-2192.
- [8] Math HJ, Bollen, Kai Yang. Harmonic aspects of wind power integration. *J. Mod. Power Syst. Clean Energy*. 2013; 1(1): 14-21.
- [9] Amirnaser Yazdani, Reza Iravani. *Voltage-Sourced Converters in Power Systems*. New Jersey: IEEE Press. 2010.
- [10] Guibin Zhang, Zheng Xu, Guangzhu Wang. *Control Strategy for Unsymmetrical Operation of HVDC-VSC based on the improved instantaneous reactive power theory*. Proceedings of the IEEE AC-DC Power Transmission international conference, London, UK. 2001; 262-267